Journal of Microscopy, Vol. 225, Pt 3 March 2007, pp. 264–268
Received 28 April 2006; accepted 17 November 2006

Micromechanical properties of tobacco mosaic viruses

ALEXANDER SCHMATULLA, NICOLA MAGHELLI & OTHMAR MARTI
Department of Experimental Physics, University of Ulm, 89069 Ulm, Germany

Key words. Atomic force microscopy, tobacco mosaic virus, Young's modulus.

Summary

A tobacco mosaic virus (TMV) subject to local forces can be viewed as an uniform beam with local loads. We used a custom built Atomic Force Microscope (AFM) to determine the curvature induced in the TMV by concentrated load or by distributed forces. Local forces were created by the AFM tip. Distributed forces were applied to the virus via the surface tension of receding droplets. The experimental results of both methods can be described when we attribute a Young modulus of 6 ± 3 GPa to the virus. Our value is about five times larger than published data. We compare our results to the literature and work out possible error sources in our experiment and in published one.

Introduction

The tobacco mosaic virus (TMV) is one of the most studied and well known viruses: its effect on plants was first described by Mayer (1886) while Ivanowski and Beijerinck recognized first the viral nature of the plant disease (Iwanowski, 1892, 1903; Beijerinck, 1898). After the first isolation and purification of the TMV by Stanley (Stanley, 1935) as soon as characterization and first X-ray studies (Bawden *et al.*, 1936) and with the advent of the electron microscope, it was possible to resolve single viral particles (Kausche *et al.*, 1939; Hibi *et al.*, 1973; Ohtsuki *et al.*, 1979; Niu *et al.*, 2006), giving a well detailed representation of the virus's molecular organization.

Despite its well-studied structure after resumption of X-ray works by F. H. C. Crick, J. D. Watson (Crick & Watson, 1956) and R. E. Franklin (Franklin & Holmes, 1958) and the recent work of B. Bhyravbhatla *et al.* (Bhyravbhatla *et al.*, 1998), rather few is yet known about its mechanical properties: owing to its simple shape, the TMV can be easily modelled as an uniform rod, making thus theoretical calculations of mechanical proper-ties such as the elastic modulus relatively easy. Moreover, its characteristic length of 282 nm and diameter of 18 nm, rather big for a virus, make the TMV an ideal candidate for Atomic Force Microscope (AFM) investigation, the only technique that can measure mechanical properties on a nm scale.

We report here qualitative and quantitative measurements of micromechanical properties of TMV.

Correspondence to: Alexander Schmatulla. e-mail: alexander.schmatulla@uni-ulm.de

Materials and methods

Viral material

The viral material investigated (common strain tobacco mosaic tobamovirus) was obtained from ATCG-LGC Promochem, Inc., catalogue number PV-135P. The original solution (1.0 mg viruses in 0.5 mL and 0.01 M sodium phosphate buffer, pH 7.2) was partitionated and stored at $-20\,^{\circ}$C. Tobacco mosaic virus, common strain, was purified from *Nicotiana tabacum* cv. *Samsun* by following the protocol of Gooding and Hebert (Gooding & Hebert, 1967).

Substrates and sample's preparation

The substrates are either freshly cleaved mica (for electron microscopy imaging and high resolution morphological analysis using tapping mode AFM) or polycarbonate ion-etched membranes (Whatman Nuclepore membranes, nominal pore diameter 220 nm). The solution consisting of TMV and ethanol (dilution 1:100) was deposited over the various substrates by means of spin coating. To preserve as much as possible the viral structure and the virus's mechanical properties, no additional treatment was applied to the viruses nor to the substrates. All the measurements have been carried out at room temperature and under ambient conditions.

Experimental setup

All AFM measurements have been made with a custom built instrument. The scanning element is a three axis piezoelectric scanner (Physik Instrumente, Model PI-517.CL,

$100 \times 100 \times 20$ micrometre scan range) driven by a low noise amplifier (Physik Instrumente, Model PI-509.C3): each axis's displacement is continuously monitored by an active feedback loop circuit to avoid creep and hysteresis (Physik Instrumente, Model PI-509.00).

The laser used to detect the lever deflection in an optical lever configuration is a single mode fiber pigtailed laser diode (Thorlabs, Model S1FC675, operated at $A = 675$ nm, $P_{out} = 0.1$ mW). The single mode fiber pigtail ensures a strictly Gaussian intensity profile that allows diffraction-limited focusing on the backside of the cantilever with an aspheric lens (Thorlabs, Model C230260P-B) matched for the numerical aperture of the optical fiber. The instrument rests on an active vibration damping table (Halcyonics, Model MOD-1) located on an air damped optical bench (Melles-Griot). A removable cover made of phonoabsorbing material encloses the instrument to provide further decoupling from ambient acoustic noise and airflows and serves also as a shield from ambient light.

The detector used to measure the reflected laser displacements is a four quadrant Si photodiode (Pacific Silicon Sensors, Model QP-50S), with its peak sensitivity around the laser's wavelength. All the driving electronics as well as the summing circuits are either custom built using surface mounted devices (SMD) or from CSEM. The data are collected by a 16 bit A/D-D/A data acquisition card (Datatranslation, Model DT3016 16 DI 16-bit channels, maximum sampling frequency 250 kHz) that synthesizes also the driving signals for the lateral scanning movements of the piezoelectric table. The data acquisition software is from Witec (Scancontrol).

Results

Tapping mode images

We used tapping mode AFM imaging to check the integrity of the viruses after the sample preparation process and before performing the force measurements. Figure 1 shows a typical 1×1 μm^2 area where viral material appears higher with respect to the mica substrate. The length of the observed object is around 700 nm, probably due to virus stacking (Drygin

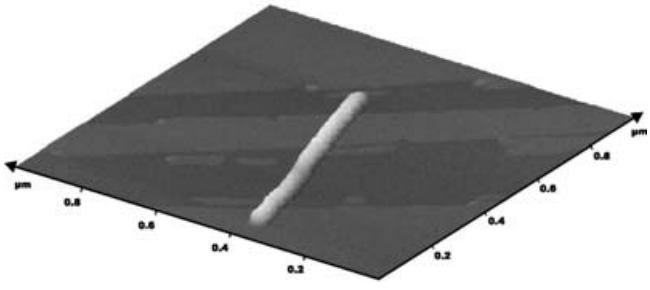

Fig. 1. High resolution AFM image (topography) of TMV in tapping mode (1×1 μm^2) on mica. Colour palette is 20 nm.

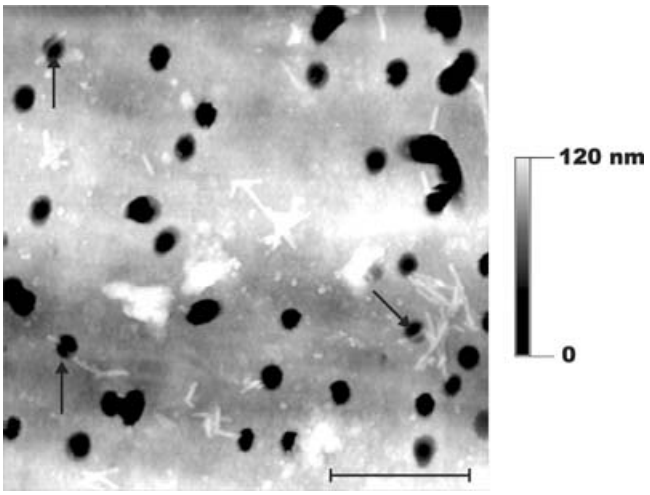

Fig. 2. Tapping mode AFM image of TMV (topography). The arrows show viruses over nanoholes. Bar size: 1000 nm.

et al., 1998). The kink in the object might be the stacking location. Tapping mode images served also to determine an optimal value for the viral concentration.

One possibility to probe the viral Young modulus is to bend a virus lying across a nanometric hole by the AFM tip. Therefore, we deposited viral material on a hydrophilic polycarbonate membrane. Figure 2 shows the topography of a sample of TMV deposited on this membranes: virus particles are clearly resolved. Some of them (marked by arrows) lie across a hole in the membrane. The height resolution in these image is not sufficient to detect any bending of the virus. The Young modulus is too high for the diameter of the holes. Figure 3 reports the corresponding phase shift image. The phase images can yield information on the material's mechanical properties

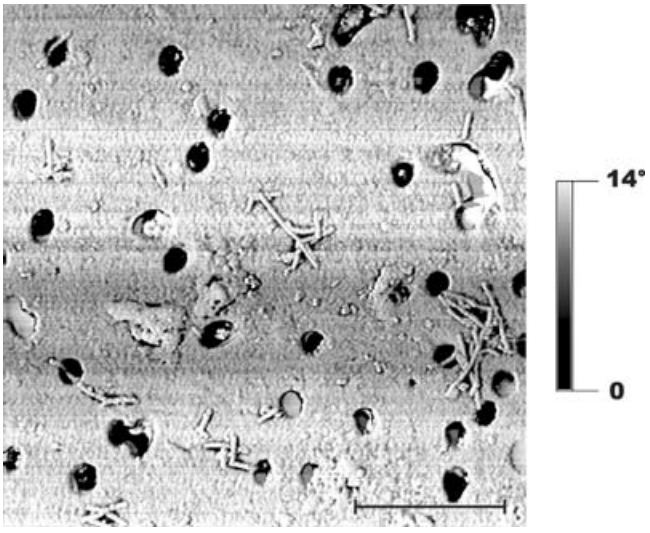

Fig. 3. Tapping mode AFM image of TMV (phase shift). Bar size: 1000 nm.

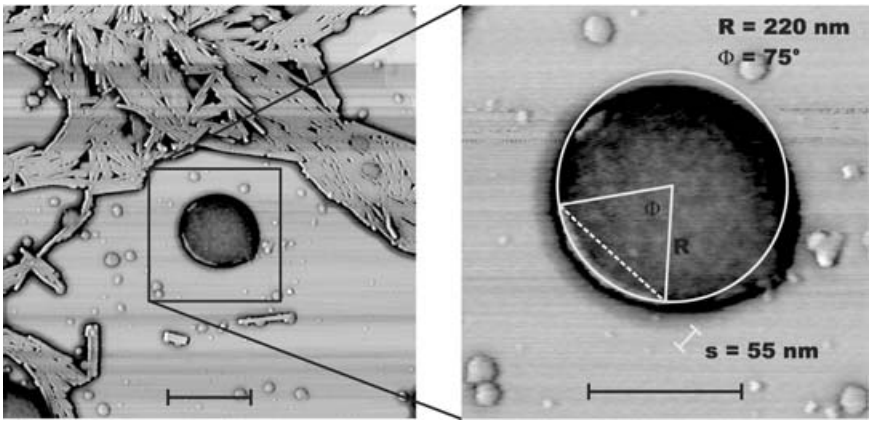

Fig. 4. Young's modulus measurement. Bar size left: 500 nm, bar size right: 300 nm.

(Winkler *et al.*, 1996; Stark *et al.*, 2001). In Fig. 3, however, very poor contrast between the virus portions lying on the polycarbonate substrate and those with a supposedly free hanging central part is visible, that is, the virus behaves under these imaging conditions like a rigid rod.

Young's modulus measurements

We were able to estimate Young's modulus of a single TMV virus from the image in Fig. 4, showing a virus particle that was found trapped inside the remain of a solvent bubble. The receding surface of the bubble bends the virus. It is deposited in this bent position when the surface of the bubble traverses it. Therefore, the virus shell shows the bending at the time where the wetting forces of the surface exceed the maximum line tension for the system solvent-virus. The Young's modulus was calculated by modelling the virus as a hollow rod and a bending momentum due to the surface tension of the solvent. The general differential equation for the displacement $u(x)$ of the virus is

$$EI\frac{d^2u(x)}{dx^2} = M(x)$$

where E is the virus's Young's module, I is the geometrical moment of inertia of the virus's cross section and $M(x)$ the applied momentum. Assuming that the virus is a hollow bar, the geometrical moment of inertia of its cross-section is

$$I = \frac{\pi}{64}\left(D_{\text{ext}}^4 - D_{\text{int}}^4\right)$$

where D_{ext} and D_{int} are the external and internal diameters, respectively. Because the diameter appears as D_4, the inner diameter D_{int} is only relevant if $D_{\text{int}} - D_{\text{ext}}$. This means, that the lack of knowledge about the structure of the inner surface does not influence the precision of the measurement. Solving the general equation for a distributed loading tension a acting over the virus's length l results in an equation relating Young's modulus E to the displacement s of the central point of the virus from its rest position (Fig. 4):

$$E = \frac{5\sigma l^4}{348sI}$$

Assuming a to be the solvent's surface tension, the calculated Young's modulus is then −6.8 GPa.

Pulsed force mode images

Pulsed force mode (PFM) imaging is an extension of AFM that allows additional quantities, such as local stiffness and adhesion, to be measured while scanning a sample. A further extension, the digital pulsed force mode (D-PFM), records for each pixel of an AFM image several force versus distance curves, allowing a much more complete analysis of the sample's mechanical properties.

Figure 5 reports the topography of a sample (TMV deposited over cleaved mica) obtained with a D-PFM module: the circled virus lays partially on the substrate and is raised at its upper end by a second virus.

Figure 6 shows two force versus distance curves obtained over the substrate and the middle point of the virus. The time required to measure the force versus distance curve is 1.0 ms. From the total elastic constant K_{tot}, measured from the fitted slope of the force–distance plot, it is possible to calculate the elastic constant of the virus K_{vir} by solving

$$E = \frac{K_{vir}l^3}{48I}\sin(\theta)$$

where K_{lever} is the cantilever's spring constant. In this configuration, the elastic constant of the virus is related to its Young's modulus E by

$$E = K_{\text{vir}}l_3\sin(6)48\,I,$$

where 0 is the angle of the virus with respect to the vertical direction (normal to the substrate's plane) and l is the length of the virus's free hanging part.

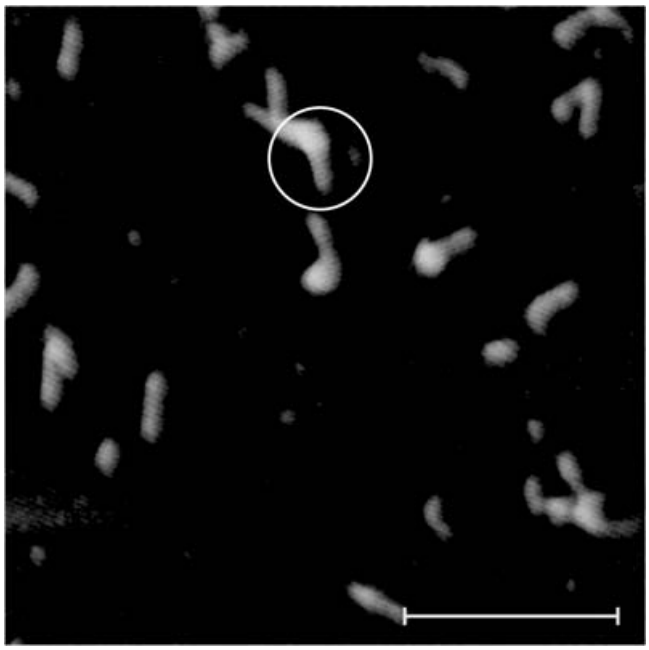

Fig. 5. Digital pulsed force mode image, topography channel. Bar size: 1000 nm, colour palette is 25 nm.

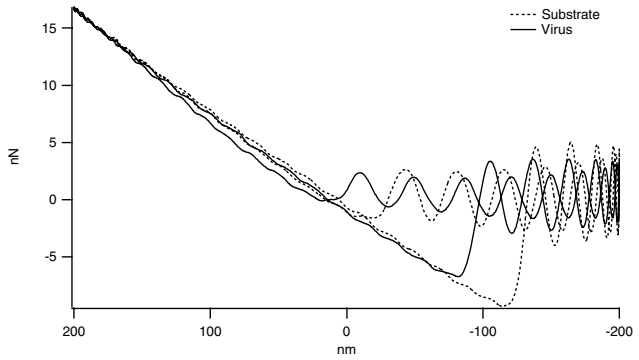

Fig. 6. Force versus distance curves on mica (dashed line) and TMV (solid).

The so calculated Young's modulus is ≈5.0 GPa at a frequency of approximately 1 kHz.

Discussion and conclusions

We measured and calculated the Young's modulus of single Tobacco Mosaic Viruses by AFM with two different methods and found consistent results. The first method is a static method ($T = 1$ s) and uses the surface tension of ethanol for bending the TMV's. The second method to measure the Young modulus is dynamic. It uses the digital pulsed force mode (D-PFM) with a repetition rate of 1000 Hz.

The trapping of viruses used for the first method only occasionally happens (Severin *et al.*, in press). Therefore, we have analyzed only two events (with same results). By calculating the surface forces due to the curvature of the droplet at the time the boundary passes the virus one gets an estimate of the static modulus of the virus. Imaging was done in intermittant contact mode to avoid changes in the curvature due to the interaction with the AFM-tip.

The alternative method uses the deviation of the deflection at different peak forces to give the modulus. Both methods give a Young modulus of 6.8 GPa (static) and 5.0 GPa (dynamic), respectively. The uncertainty of the measurement is mostly systematic (lack of knowledge of the radius of curvature of the tip and of the compliance of the cantilever). Since we use point like force in the analysis, the unknown tip shape does not change the ratio of the values obtained by the dynamical method. We estimate the systematic error for the static method to be ±2.4 GPa and the systematic error for the dynamic method to be ±3.8 GPa. Taking into account the errors, we still find that our results are of the order of 5 larger than published values (Guthold *et al.*, 1999), a factor of 2 stiffer as Poly(methyl methacrylate) (Plexiglas) with a Young modulus of 3.3 GPa (Brandrup & Immergut, 1989). The advantage of our virus bending methods is that we can ignore adhesion forces between virus and substrate. In the first method, the virus is suspended in the liquid until its shape is frozen on the surface. The second method is based on the difference of the bending when applying an additional point like force. This additional bending is independent to first order from the size of the constant load. Other approaches (Falvo *et al.*, 1997) have assumed that the shear stress between graphite and the protein coat (capsid) of the TMV is compararable with the shear stress of molybdenum sulfide (solid lubricant). A further uncertainty in their method is the real unknown contact area and not well-known adhesion forces between the virus and the graphite surface while dragging. Such assumptions are not necessary for our approach. If we compare our results with the Young modulus of microtubules of 2 GPa measured by other research groups (Kis *et al.*, 2002; Kasas *et al.*, 2004a,b), a TMV is stiffer by a factor of 3. In comparison to a bulk polymer, for example, isotactic polypropylene, with a well-known Young modulus between 1 and 1.7 GPa (Brandrup and Immergut, 1975), a TMV is approximately stiffer by a factor of 5. The protein subunits (capsid) determine the helical shape. Intermolecular non-covalent bondings between the protein molecules and between the protein molecules and the RNA build a framework which is decisive for the high stiffness of a TMV. The high virus stability derives directly from the densely packed structure of the virus particles in the layer structure (Bhyravbhatla *et al.*, 1998). We have shown a reliable method to determine not only the material properties of TMV but also for microtubules (de Pablo *et al.*, 2003), actin filaments, amyloid fibers (Kammerer *et al.*, 2004) or other biological or chemical filaments. Future developments will be an increasing of the lateral resolution during the virus bending, especially in digital pulsed force mode.

Acknowledgements

One of us (NM) gratefully acknowledge financial support by the DFG via the SFB 569, project C1. Sample preparation was done by our biological-technical assistant Ulla Nolte. The authors gratefully acknowledge Martin Pietralla, Bernd Heise, Gerd-Ingo Asbach, Sabine Hild, Paul Walther and especially Matthias Freyberger for their lively interests and scientific discussions.

References

Bawden, F.C., Pirie, N.W., Bernal, J.D. & Fankuchen, I. (1936) Liquid crystalline substances from virus-infected plants. *Nature* **138**, 1051–1052.

Beijerinck, M.W. (1898) Ueber ein Contagium Vivum Fluidum als Ursache der Fleckenkrankheit der Tabacksblaetter. Verh. *Kon. Akad.* **5**, 3–21.

Bhyravbhatla, B., Watowich, S.J. & Caspar, D.L.D. (1998) Refined atomic model of the four-layer aggregate of the tobacco mosaic virus coat protein at 2.4 A*A* resolution. *Biophys. J.* **74**, 604–615.

Brandrup, J. & Immergut, E. H. (1975) *Polymer Handbook*. Wiley & Sons.

Brandrup, J. & Immergut, E.H. (1989) *Polymer Handbook*. Wiley & Sons, New York, USA.

Crick, F.H.C. & Watson, J.D. (1956) Structure of small viruses. *Nature* **177**, 473–475.

Drygin, Yuri F., Bordunova, Olga A., Gallyamov, Marat O. & Yaminsky, Igor V. (1998) Atomic force microscopy examination of tobacco mosaic virus and virion rna. *FEBS Lett.* **425**, 217–221.

Falvo, M.R., Washburn, S., Superfine, R., Finch, M., Brooks, F.P. Jr., Chi, V. & Taylor, R.M. II (1997) Manipulation of individual viruses: friction and mechanical properties. *Biophys. J.* **72**, 1396–1403.

Franklin, R.E. & Holmes, K.C. (1958) Tobacco mosaic virus: application of the method of isomorphous replacement to the determination of the helical parameters and radial density distribution. *Acta Csyst.* **11**, 213–220.

Gooding, G.V. & Hebert, T.T. (1967) A simple technique for purification of tobacco mosaic virus in large quantities. *Phytopathology* **57**, 1285.

Guthold, M., Falvo, M.R., Matthews, W.G. *et al.* (1999) Investigation and modification of molecular structures with the nanomanipulator. *J. Mol. Graph. Model.* **17**, 187–197.

Hibi, T., Yada, K., Takahashi, S. & Shibata, K. (1973) High resolution electron microscopy of tobacco mosaic virus. *J. Electron Microscopy* **22**, 243–253.

Iwanowski, D. (1892) Concerning the mosaic disease of the tobacco plant. *St. Petersb. Acad.Imp. Sci. Bul.* **35**, 67–70.

Iwanowski, D. (1903) Ueber die Mosaikkrankheit der Tabakspflanze. *Zeit.* Pflanzenkr. Pflanzenpathol. Pflanzenschutz **13**, 1–41.

Kammerer, R.A., Kostrewa, D., Zurdo, J. *et al.* (2004) Exploring amyloid formation by a de novo design. *Proc. Natl. Acad. Sci. U.S.A.* **101**, 4435–4440.

Kasas, S., Kis, A., De Los Rios, P., Riederer, B.M., Forr´o L., Dietler, G. & Catsicas, S. (2004a) Oscillation modes of microtubules. *Biology of the Cell* **96**, 697–700.

Kasas, S., Kis, A., Riederer, B.M., Forr´o, L., Dietler, G. & Catsicas, S. (2004b) Mechanical properties of microtubules explored using the finite elemente method. *Chem. Phys. Chem.* **5**, 252–257.

Kausche, G.A., Pfankuch, E. & Ruska, A. (1939) Die Sichtbarmachung von pflanzlichem Virus im Uebermikroskop. *Naturwissenschaften* **27**, 292–299.

Kis, A., Kasas, S., Babi´c, Kulik, A.J. *et al.* (2002) Nanomechanics of microtubules. *Phys. Rev. Lett.* **89**, 248101-1–248101-4.

Mayer, A. (1886) Ueber die Mosaikkrankheit des Tabak. *Landwirtsch. Vers.* **32**, 451–467.

Niu, Z., Bruckman, M., Kotakadi, V.S. *et al.* (2006) Study and characterization of tobacco mosaic virus head-to-tail assembly assisted by aniline polymerization. *Chem. Commun.*, 3019-3021.

Ohtsuki, M., Isaacson, M.S. & Crewe, A.V. (1979) Dark field imaging of biological macromolecules with the scanning transmission electron microscope. *Proc. Natl. Acad. Sci. U.S.A.* **76**, 1228–1232.

de Pablo, P.J., Schaap, I.A.T., MacKintosh, F.C. & Schmidt, C.F. (2003) Deformation and collapse of microtubules on the nanometer scale. *Phys. Rev. Lett.* **91**, 098101-1–098101-4.

Severin, N., Zhuang, W., Ecker, C., Kalachev, A.A., Sokolov, I.M. & Rabe, J.P. Blowing DNA bubbles. *Nanoletters*, in press.

Stanley, W.M. (1935) Isolation of a crystalline protein possesing the properties of tobacco mosaic virus. *Science* **81**, 644–645.

Stark, M., Moeller, C., Mueller, D.J. & Guckenberger, R. (2001) From images to interactions: high-resolution phase imaging in tapping-mode atomic force microscopy. *Biophys. J.* **80**, 3009–3018, June.

Winkler, R.G., Spatz, S., Sheiko, M., Moeller, M., Reineker, P. & Marti, O. (1996) Imaging material properties by resonant tapping-force microscopy: a model investigation. *Phys. Rev. B* **54**, 8908–8912.